

AD-A217 073

(E (When Date Entered))

②

## NTATION PAGE

READ INSTRUCTIONS  
BEFORE COMPLETING FORM

• ARO 23808.3-MS-F

2. GOVT ACCESSION NO

NA

3. RECIPIENT'S CATALOG NUMBER

NA

## 4. TITLE (and Subtitle)

NMR Imaging Development for the study of Solids

## 5. TYPE OF REPORT &amp; PERIOD COVERED

Final 27 Aug '86  
17 Nov 89

## 6. PERFORMING ORG. REPORT NUMBER

## 7. AUTHOR(s)

B. H. Suits  
Physics Dept., Michigan Tech Univ.

## 8. CONTRACT OR GRANT NUMBER(s)

DAAL03-86-G-0065

## 9. PERFORMING ORGANIZATION NAME AND ADDRESS

Physics Dept  
Michigan Technological University  
Houghton, Mi 4993110. PROGRAM ELEMENT, PROJECT, TASK  
AREA & WORK UNIT NUMBERS

NA

## 11. CONTROLLING OFFICE NAME AND ADDRESS

U. S. Army Research Office  
P. O. Box 12211  
Research Triangle Park, NC 27709-2211

## 12. REPORT DATE

20 December 1989

## 13. NUMBER OF PAGES

9

## 14. MONITORING AGENCY NAME &amp; ADDRESS (if different from Controlling Office)

## 15. SECURITY CLASS. (of this report)

UNCLASSIFIED

15a. DECLASSIFICATION/DOWNGRADING  
SCHEDULE

## 16. DISTRIBUTION STATEMENT (of this Report)

Approved for public release; distribution unlimited.

## 17. DISTRIBUTION STATEMENT (of the abstract entered in Block 20, if different from Report)

NA

## 18. SUPPLEMENTARY NOTES

The view, opinions and/or findings contained in this report are those of the author(s) and should not be construed as an official Department of the Army position, policy, or decision, unless so designated by other documentation.

## 19. KEY WORDS (Continue on reverse side if necessary and identify by block number)

NMR Imaging Solids  
Non-destructive evaluation (NDE)  
Defects in solids  
Non-invasive measurements

## 20. ABSTRACT (Continue on reverse side if necessary and identify by block number)

The Techniques of NMR imaging are developed for simple inorganic solids and applied to the study of mechanically induced defects in NaCl. The feasibility of the technique is demonstrated for defect (dislocation) densities greater than  $10^7/\text{cm}^2$  with a resolution of better than 1mm.

90 01 23 189

DTIC FILE COPY

DTIC  
ELECTE  
JAN 24 1990  
S E D

NMR Imaging Development for the Study of Solids

Final Report

B. H. Suits

20 December 1989

U.S. Army Research Office

Grant: DAAL03-86-G-0065

Physics Dept.  
Michigan Technological University  
Houghton, Michigan

Accession For	
NTIS GRA&I	<input checked="" type="checkbox"/>
DTIC TAB	<input type="checkbox"/>
Unannounced	<input type="checkbox"/>
Justification	
By	
Distribution/	
Availability Codes	
Dist	Avail and/or Special
A-1	

Approved for Public release; Distribution Unlimited

ABSTRACT: The Techniques of NMR imaging are developed for simple inorganic solids and applied to the study of mechanically induced defects in NaCl. The feasibility of the technique is demonstrated for defect (dislocation) densities greater than  $10^7/\text{cm}^2$  with a resolution of better than 1  $\mu\text{m}$ .

The view, opinions, and/or findings contained in this report are those of the author and should not be construed as an official department of the army position, policy, or decision, unless so designated by other documentation.

### Problem Studied

This grant covered, in part, the cost of one graduate student working on the NMR imaging of solids in conjunction with research sponsored by the US ONR under grants N00014-86-K-0149 and N00014-86-C-0724 subcontract SK&OD7820F from Lockheed corporation.

The goal of the research was to:

- i) Improve the quality of NMR images obtained from simple inorganic solids so they are useful non-destructive, non-invasive tools to study mechanically induced defects in solids.
- ii) Use the techniques on mechanically damaged materials to establish the utility of the technique to study mechanically damaged materials.

### Summary of Most Important Results

The quality of images using the  $^{23}\text{Na}$  signal from NaCl in a propellant simulant has improved as a function of time, as is illustrated in figure 1. The image labeled "1989" is, in fact, of high enough resolution that the use of contour plots is misleading. The images are normally viewed on the computer screen however a simple cost-effective means of reproducing these images has not been found. The major improvements to the equipment are the increase in gradient strength used to form the image and some improvements in the software data processing. The details of these improvements has been previously reported (see semi-annula progress reports, this grant).

The contents of the propellant simulant are shown in table I. The improvements in our instrumentation were sufficient that we were able to obtain a usable image using the Aluminum signal from the metal particles in the simulant. This image is shown in figure 2. The aluminum NMR signal is several times broader than the Na signal making images that much more difficult to obtain. To the best of our knowledge, no one has obtained a better image using aluminum with any technique. Attempts at Lockheed corporation to use sophisticated multiple pulse techniques did not yield an improved resolution due to significant distortions from off resonance signals.

The utility of the NMR imaging technique to study damaged materials was demonstrated and is contained in the reprint which is appendix A of this report. It is important to note that the line narrowing techniques commonly used for solids work cannot be used to study quadrupole broadened NMR signals to study defects. The line narrowing techniques reduce or remove the effects of the defects on the NMR signal. Our work so far has concentrated on the non-destructive measurement of defect densities in mechanically damaged NaCl using the NMR signal from the Na nucleus. The results demonstrate the utility of the technique to study mechanically damaged materials using the non-invasive NMR imaging technique.

Publications (this grant)

- "Nuclear Magnetic Resonance Imaging as a Tool to Characterize Defect Densities in Solids," B. H. Suits and J. L. Lutz, J. Appl. Physics 65, 3728 (1989).

Participating Scientific Personnel

B. H. Suits (PI)

J. L. Lutz, MS 1989 (through summer 1989)

D. E. Wilken, (starting summer 1989 on this grant, MS 1988)

Figure 1

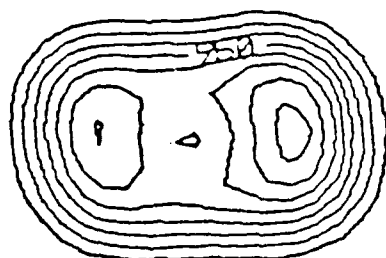


# Resolution versus Time PBAN propellant simulant

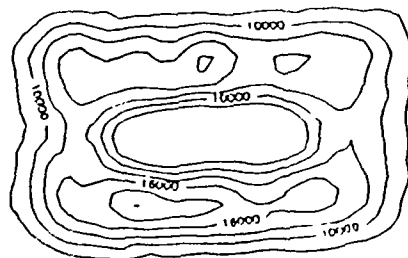
NMR IMAGES  
as contour plots

SAMPLE GEOMETRY

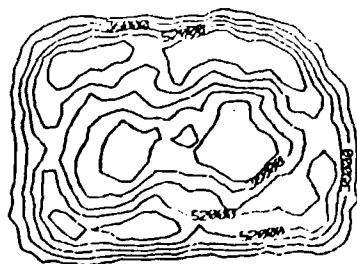
1987



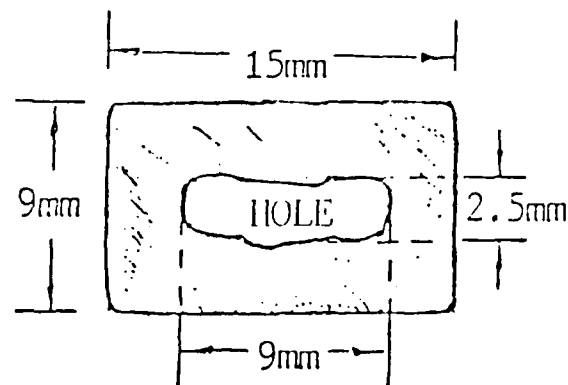
1988



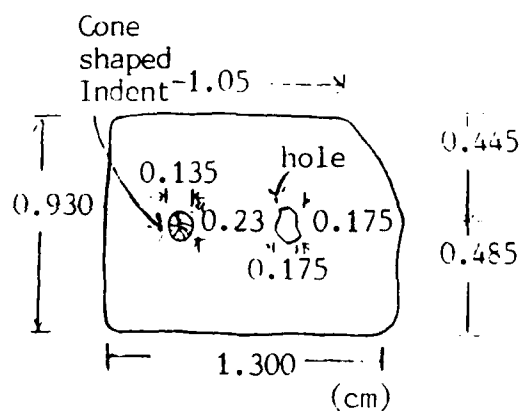
1989



Note: New sample with more detail



(1mm thick)



<sup>23</sup>Na from solid NaCl

(Actual resolution is very dependent on the particular situation studied and care must be used when comparing these results to other results on different materials)

Figure 2

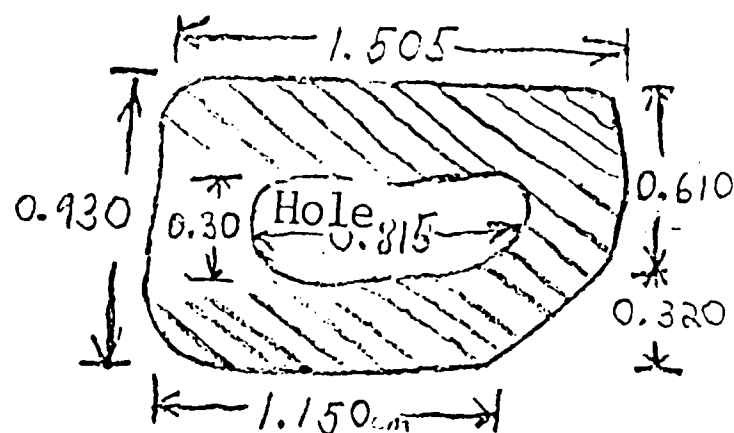
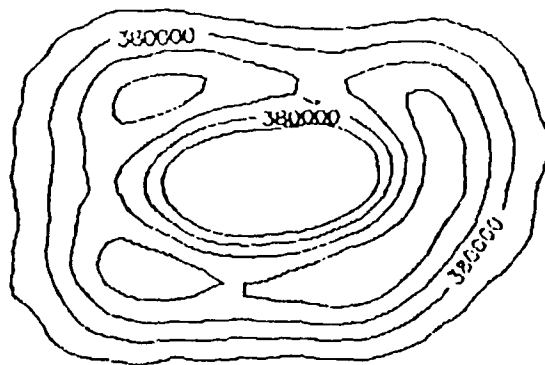


$^{27}\text{Al}$  signal

NMR IMAGES

Sample Dimensions

1989



(1 mm thick)

PBAN Propellant Simulant  
(contains Al Particles)

## PBAN Propellant Simulant

<u>Component</u>	<u>weight %</u>
PBAN	14
Al (powder)	16
NaCl	49
$(\text{NH}_4)_2\text{SO}_4$	21

# Nuclear magnetic resonance imaging as a tool to characterize defect densities in solids

B. H. Suits and J. L. Lutz

Physics Department, Michigan Technological University, Houghton, Michigan 49931

(Received 23 September 1988; accepted for publication 13 January 1989)

Nuclear magnetic resonance imaging methods demonstrate the spatial variation of  $^{23}\text{Na}$  signal intensity in NaCl which results from an impact-induced inhomogeneous defect distribution.

Nuclear magnetic resonance (NMR) imaging of solids is a relatively new, nondestructive, noninvasive measurement technique which has been shown to be useful in monitoring inhomogeneities of chemical species,<sup>1,2</sup> and for identifying cracks in materials.<sup>1,3</sup> The work presented here demonstrates the utility of the technique to study the spatial distributions of other types of material defects as well, in particular, dislocations in solids containing a nucleus with a nonzero quadrupole moment.

The use of NMR to study mechanically induced defects is not new.<sup>4</sup> A comprehensive review of the effects on the quadrupole interaction due to point defects and dislocations in cubic systems has been presented by Kanert and Mehring.<sup>5</sup> What is new here is the application of these ideas in a spatially resolved mode.

This discussion is limited to the use of the electric quadrupole interaction, though other interactions which are modified in the presence of defects may prove useful as well. Thus, the discussion is limited to nuclei with spin,  $I > 1/2$ .

The electric quadrupole interaction is due to the presence of an electric field gradient (efg) at the nucleus under study which couples to the nuclear electric quadrupole moment ( $eQ$ ). The quadrupole interaction is discussed in detail elsewhere.<sup>6-8</sup> The efg can be described using a symmetric, traceless, second-rank tensor  $V$  with components  $V_{\alpha\beta}$  ( $\alpha, \beta = x, y, z$ ). The tensor represented using one coordinate system ( $x_1, x_2, x_3$ ) can be transformed to another ( $x'_1, x'_2, x'_3$ ) using the rotation

$$V^{(x')} = T^{-1} V^{(x)} T, \quad (1)$$

where the elements of  $T$ ,  $T_{ij}$ , are the cosines of the angles between  $x'_i$  and  $x_j$ . It is convenient to discuss the efg in a reference frame where  $V_{\alpha\beta} = 0$  if  $\alpha \neq \beta$ , known as the principle axis system.

For NMR measurements in a high magnetic field  $H$ , it is often the case that the Zeeman interaction, described by the Hamiltonian  $\mathcal{H}_z = -\gamma\hbar\mathbf{H} \cdot \mathbf{I}$ , where  $\gamma$  is the gyromagnetic ratio and  $\mathbf{I}$  is a spin operator, is large compared to the quadrupole interaction,  $\mathcal{H}_Q$ . If the convention is used that the magnetic field  $H$  is along the  $z$  axis of the lab frame ( $x, y, z$ ) and the principle axes of  $\mathcal{H}_Q$  define a crystal reference frame ( $x', y', z'$ ), then (to first order in perturbation theory) one has a total interaction described by the Hamiltonian  $\mathcal{H}$ :

$$\mathcal{H} = -\gamma\hbar H I_z + [eQ/4I(2I-1)][3I_z^2 - I^2] V_{zz}, \quad (2)$$

where, using Eq. (1),

$$V_{zz} = V_{xx} \cos^2 \theta + V_{xx} \sin^2 \theta \cos^2 \phi + V_{yy} \sin^2 \theta \sin^2 \phi, \quad (3)$$

where  $\theta$  and  $\phi$  are the Euler angles relating the primed to the unprimed coordinates. This yields magnetic dipole transition frequencies  $\omega_m$  between the states characterized by  $m$  and  $m+1$ ,  $m = -I, -I+1, \dots, I$ ,

$$\omega_m = \gamma H + [3eQ/8I(2I-1)\hbar](2m+1)V_{zz}. \quad (4)$$

Note that the transition from  $m = -\frac{1}{2}$  to  $m = +\frac{1}{2}$  (present for nuclei with half-integer spin) is not sensitive in first order to the presence of the quadrupole interaction, while other transitions can be strongly affected.

There are many types of defects in materials.<sup>9-10</sup> Associated with any defect is a strain field, the nature of which depends on the particular type of defect. The distance over which these strain fields have an impact on the NMR signal may be quite large.

For simplicity, the details of only one type of defect, an isolated dislocation, will be presented here. The features which emerge for others are qualitatively similar.

It is quite difficult to treat nuclei which are very close to the defect, but outside this "core" region elastic theory can be used. Estimates of the size of the core region show that it is only a few lattice constants in radius.<sup>10</sup>

In the region where the elastic theory applies the atoms will be displaced only a small amount relative to their neighbors and hence one can assume that the changes in the quadrupole interaction will be linearly related to the local strain,  $\epsilon$ , or stress,  $\sigma$ . With this assumption one can write

$$V_{ij} = V_{ij}^0 + \sum_{k,l} C_{ijkl} \sigma_{kl}. \quad (5)$$

The coefficients  $C_{ijkl}$  are measured quantities and values for many cubic systems are tabulated in Ref. 5.

A dislocation is characterized by a line through the material and a slip plane. If the dislocation line defines the  $z''$  axis and the slip plane lies in the  $x''-z''$  plane, then the stress tensor for a screw dislocation is

$$\sigma'' = \frac{Gb}{2\pi r} \begin{pmatrix} 0 & 0 & -\sin \theta \\ 0 & 0 & \cos \theta \\ -\sin \theta & \cos \theta & 0 \end{pmatrix} \quad (6)$$

and for the edge dislocation



$$\sigma'' = \frac{D}{r} \begin{pmatrix} -\sin \theta (2 + \cos 2\theta) & \cos \theta \cos 2\theta & 0 \\ \cos \theta \cos 2\theta & \sin \theta \cos 2\theta & 0 \\ 0 & 0 & 2\nu \sin \theta \end{pmatrix}, \quad (7)$$

where  $G$  is the shear modulus,  $b$  is the magnitude of the Burgers vectors,  $D = Gb/[2\pi(1-\nu)]$  where  $\nu$  is the Poisson ratio and the  $r$  and  $\theta$  are the positions in the sample relative to the dislocation in the dislocation's reference frame. Thus, the efg in the lab reference frame can be calculated as

$$V = T^{-1}U^{-1}(V^0 + C\sigma)UT, \quad (8)$$

where  $U$  transforms the interaction from the double prime to prime coordinates and  $T$  into the laboratory frame.

It can be seen that both types of dislocations yield an angularly dependent response. In some cases this angular dependence can be used as a means of characterizing the defects which are present.

Due to the cubic symmetry at the  $^{23}\text{Na}$  site in NaCl the efg tensor in the undistorted lattice,  $V^0$ , is zero and all the transitions occur at the same frequency,  $\gamma H/\hbar$ . As an explicit example, the screw dislocation in NaCl [(110)(110) slip system] gives

$$V_{zz} = (GbC_{11}/2\pi r)f(\theta, T, U).$$

The function  $f(\theta, T, U)$  (see Ref. 5) describes the angular dependence and in this case has the property that it is zero if the magnetic field is along or perpendicular to the dislocation. Putting in numbers one has an additional splitting of the  $I = \pm \frac{3}{2}$  to  $\pm \frac{1}{2}$  transition given approximately by

$$\Delta\nu = \pm (2.4 \text{ MHz}/r)f(\theta, T, U), \quad (9)$$

where  $r$  is the distance from the dislocation line in angstroms. Figure 1 illustrates the effects of the dislocation on the NMR signal. Curves of constant frequency shift of the  $\pm \frac{3}{2}$  to  $\pm \frac{1}{2}$  satellite transition appear as lobes about the dislocation.

In the core region one does not know the efg but the number of nuclei involved is quite small and this region can be ignored. Outside the core region is a region where the quadrupole shift moves the satellites outside the bandwidth

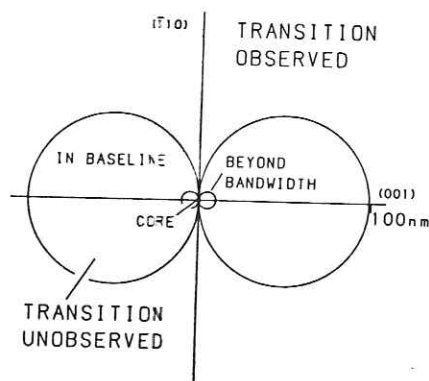


FIG. 1. A schematic diagram of the spatial dependence of the contribution to the NMR signal from the  $\pm \frac{3}{2}$  to  $\pm \frac{1}{2}$  satellite transitions near a dislocation. The figure is scaled appropriately for the  $^{23}\text{Na}$  signal from NaCl with the magnetic field along (100).

of the spectrometer (in our case roughly 0.3 MHz). The signal from these regions will be reduced in two ways: (1) the  $\pm \frac{3}{2}$  to  $\pm \frac{1}{2}$  transitions will be missing and (2) the  $-\frac{1}{2}$  to  $+\frac{1}{2}$  transition will be decreased in magnitude due to the fact that it must be treated in the effective spin  $\frac{1}{2}$  approximation.<sup>6</sup> Outside this region is a region labeled "in baseline." From a simple point of view one regards the satellite transition frequencies from this region to be spread out over such a wide range that the total response within the spectrometer bandwidth is effectively flat. These signals are observed in a rigorous sense but if the baseline is corrected before or during image processing, they are removed. All that is observed then is the  $-\frac{1}{2}$  to  $\frac{1}{2}$  transition.

Outside all these regions the shift is small compared to the NMR linewidth (in this case roughly 3 kHz) and hence the effects of the dislocation are obscured and the full intensity is observed.

Of course, the dividing lines between the regions are not sharp and there is some change in the central lineshape used to create the image. The changes in lineshape are not overwhelming and this simple picture reflects the essence of the behavior.

The sensitivity of the NMR technique is quite good. Using the estimated 100 nm as the maximum range of the effects of the dislocation then in a cross section one has rough-

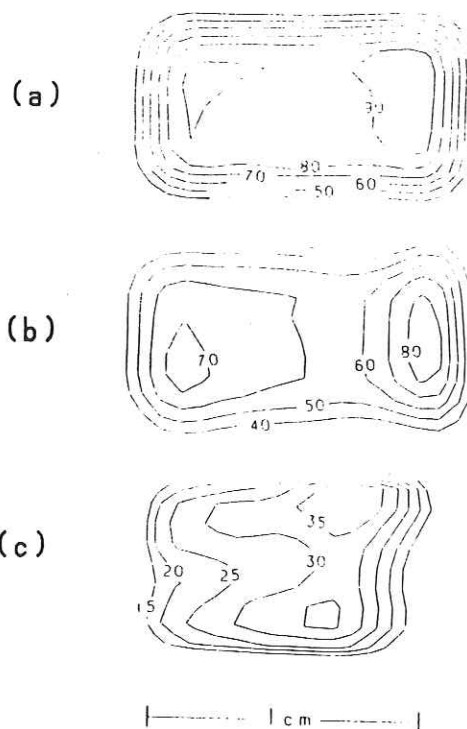


FIG. 2. NMR images showing the spatial distribution of the NMR intensity (a) before and (b) after extensive damage to part of the crystal by impact. The difference (percent) between (a) and (b) is shown in (c). The change in signal intensity is due to the presence of defects which alter the NMR response. The sample is  $1 \times 0.54 \text{ cm}^2$  and 0.2 cm thick. The view is through the thickness of the sample.

ly  $1.6 \times 10^{-10} \text{ cm}^3$  which is unobserved for each dislocation. Thus, dislocation densities larger than about  $10^6$  or  $10^7/\text{cm}^2$  should be observable in NaCl using this technique for measurements with a good signal to noise ratio.

Figure 2 shows images for a crystal which has been damaged by impact using a drop hammer (495 g from 9 cm high). These images are two-dimensional projections through the thickness of the sample with the strike along the direction of view. Part of the sample (the right-most quarter in Fig. 2) was outside the region of the strike. The damage is clearly evident as a large decrease in intensity in the region that was hit. Plastic deformation of the damaged region is roughly 5% (there was no measureable loss of mass).

Figure 3 shows cross sections through the center for two orientations of the damaged crystal with respect to the applied magnetic field. The view of the sample is the same in both cases. There is a significant difference which is not uniform from one side of the sample to the other. That is, the defect distribution as seen by the  $^{23}\text{Na}$  nuclei does not have the cubic symmetry of the host lattice and the degree to which the symmetry is broken varies across the sample. One way the symmetry can be broken is if there are more dislocations along one direction than another equivalent direction. In cases where the defect density is high and a nucleus can "see" more than one at a time (for NaCl a local density of roughly  $10^{10}/\text{cm}$  or greater), a difference in the microscopies of the distribution for different directions may also give rise to this effect. As a simple example, if in one direction the dislocations occur in bunches, whereas in another they are spread out uniformly, one can expect this phenomena. It should be noted that the original sample, which was cleaved from a larger melt-grown block, also showed a lack of cubic symmetry for the NMR response, however, in this case the change in signal intensity upon rotation of the magnetic field was uniform across the sample. The observed lack of cubic symmetry in the undamaged sample is not unexpected based on previous results for NaCl.<sup>5</sup>

The NMR data presented in this paper was obtained using a "homemade" microcomputer controlled NMR spectrometer with a magnetic field of approximately 85 kG (360 MHz for protons, 95 MHz for  $^{23}\text{Na}$ ). The projection reconstruction (convolution backprojection) algorithm described in Ref. 1 was used to create images from Fourier transformed free induction decays. The gradient strength used for images was approximately 15 G/cm. In all of these images, the linear resolution is limited by the NMR linewidth to about 1 mm.

The imaging method used so far in these studies has been the bare minimum. With improvements in the technique one can hope to improve the sensitivity and resolution of the images and to streamline the analysis of the defects present.

These results show that NMR imaging can be used to measure, and to some extent characterize, defect distribu-

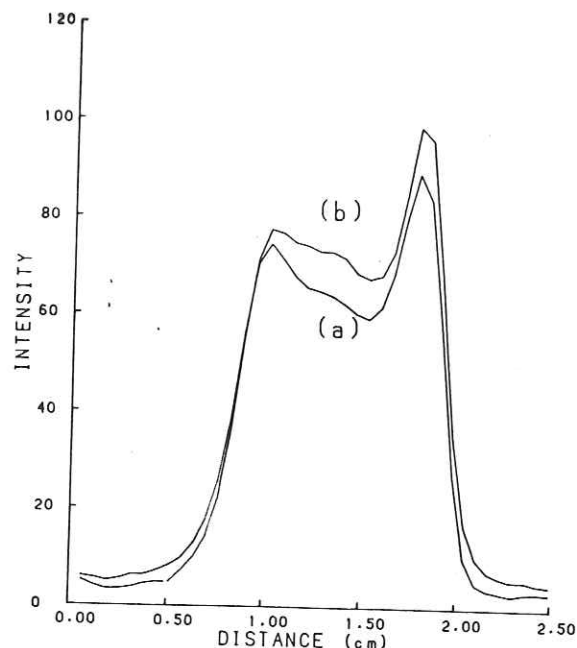


FIG. 3. Cross sections through images of the heavily damaged crystal for two orthogonal orientations of the magnetic field; magnetic field (a) perpendicular and (b) parallel to the sample face. The defect distribution does not have the cubic symmetry of the NaCl lattice and hence destroys the cubic symmetry of the NMR response.

tions in solids. The NMR imaging technique complements existing techniques which allow one to visualize individual defects. The advantage of NMR imaging over these techniques is that one can see into the interior of a sample, independent of the material's opacity, in a noninvasive way. In an industrial setting, such as for the manufacture of explosives, NMR imaging has some obvious advantages.

This work was supported in part by the U.S. Office of Naval Research and the U.S. Army Research Office.

<sup>1</sup>B. H. Suits and D. White, *Solid State Commun.* **50**, 291 (1984).

<sup>2</sup>For example, see G. C. Chingas, J. B. Miller, and A. N. Garroway, *J. Magn. Reson.* **66**, 530 (1986), and references therein.

<sup>3</sup>B. H. Suits and D. White, *J. Appl. Phys.* **60**, 3772 (1986).

<sup>4</sup>G. D. Watkins and R. V. Pound, *Phys. Rev.* **89**, 658 (1953).

<sup>5</sup>O. Kanert and M. Mehring, In *NMR—Basic Principles and Progress*, edited by P. Diehle, E. Fluck, and R. Kosfeld (Springer, Berlin, 1971), Vol. 3; see also J. Th. M. De Hosson, O. Kanert, and A. W. Sleeswyk, in *Dislocation in Solids*, edited by F. R. N. Nabarro (North-Holland, Amsterdam, 1983), Vol. 6, Chap. 32.

<sup>6</sup>A. Abragam, *Principles of Nuclear Magnetism* (Oxford, London, 1961).

<sup>7</sup>T. P. Das and E. L. Hahn, *Solid State Physics, Supplement 1* (Academic Press, New York, 1958), Vol. 1, p. 3ff.

<sup>8</sup>C. P. Slichter, *Principles of Magnetic Resonance*, 2nd ed. (Springer, Berlin, 1978).

<sup>9</sup>J. Friedel, *Dislocations* (Pergamon, New York, 1964).

<sup>10</sup>J. J. Gilman, General Electric Research Laboratory Report 59-RL-2194, 1959.